Hindawi
Journal of Nanomaterials
Volume 2021, Article ID 6652648, 8 pages
https://doi.org/10.1155/2021/6652648

Research Article

Evaluation of Inflammatory and Calcification after Implantation of Bioabsorbable Poly-L-Lactic Acid/Amorphous Calcium Phosphate Scaffolds in Porcine Coronary Arteries

Gaoke Feng,[1,2,3] **Chaoshi Qin**,[4] **Fei Sha**,[5] **Yongnan Lyu**,[1,2,3] **Jinggang Xia**,[6] **and Xuejun Jiang**[1,2,3]

[1]*Department of Cardiology, Renmin Hospital of Wuhan University, Wuhan 430060, China*
[2]*Cardiovascular Research Institute, Wuhan University, Wuhan 430060, China*
[3]*Hubei Key Laboratory of Cardiology, Wuhan 430060, China*
[4]*Department of Cardiology, Tangdu Hospital, Fourth Military Medical University, Xi'an 710038, China*
[5]*Department of Vascular Surgery, Wang Jing Hospital, China Academy of Chinese Medical Sciences, Beijing 100102, China*
[6]*Department of Cardiology, Xuanwu Hospital, Capital Medical University, Beijing 100053, China*

Correspondence should be addressed to Gaoke Feng; 123fgk@163.com and Xuejun Jiang; xjjiang@tom.com

Received 1 November 2020; Revised 1 January 2021; Accepted 9 January 2021; Published 23 January 2021

Academic Editor: Luis Jesús Villarreal-Gómez

Purpose. Our previous research has confirmed that the addition of nano-amorphous calcium phosphate (ACP) materials can improve the support of poly-L-lactic acid (PLLA) vascular scaffolds. Based on this, we continued to explore the effect of novel bioresorbable scaffold composed of PLLA and ACP nanoparticles on inflammation and calcification of surrounding tissues after scaffold implantation in porcine coronary artery. *Methods*. PLLA/ACP scaffolds in the experimental group and PLLA scaffolds in the control group were implanted into the coronary arteries of small pigs. Serum levels of C-reactive protein (CRP), calcium (Ca), and alkaline phosphatase (ALP) were measured before implantation and at 1, 6, 12, and 24 months after operation. Intravascular ultrasonography (IVUS) was performed to evaluate the vascular calcification score. The scaffold and surrounding tissues were hematoxylin-eosin staining for inflammation score. The scaffold and surrounding tissues were stained with NF-κB and ALP, and the positive expression index was calculated. Western blot was used to detect the expression of IL-6 and BMP-2 in the tissues around the scaffold. *Results*. There was no statistically significant difference between the two groups in CRP, calcium, and ALP at preimplant, 1 month, 6 months, 12 months, and 24 months ($P > 0.05$). The inflammation score, NF-κB positive expression index, and calcification score in the PLLA/ACP group were lower than that in the PLLA group at 12 months and 24 months ($P < 0\,05$). The ALP positive expression index in the PLLA/ACP group was lower than that in the PLLA group at 6 months, 12 months, and 24 months ($P < 0\,05$). Western blot results showed that the IL-6 expression level in the PLLA/ACP group was significantly lower than that in the control group at 6 months, 12 months, and 24 months ($P < 0.05$). The expression of BMP-2 in the PLLA/ACP group was significantly lower than that in the control group at 12 months and 24 months ($P < 0.05$). *Conclusion*. The PLLA/ACP composite scaffold has good biocompatibility. The incorporation of nanoscale ACP can reduce the inflammatory response caused by the acid metabolites of PLLA scaffolds, reduce the expression of procalcification factors in the body, and inhibit tissue calcification. The PLLA/ACP composite scaffold provides reliable guidance for the application and development of degradable vascular scaffold.

1. Introduction

Bioabsorbable scaffold is the mainstream direction of interventional therapy for coronary heart disease. At present, the bioabsorbable scaffolds represented by PLLA have a promising prospect in clinical practice on the basis of their biodegradable ability and support performance. However, poly-L-lactic acid material (PLLA) has its own limitations,

and its support performance is less than that of metal scaffold [1, 2]. Besides, during the degradation of PLA materials in vivo, it may produce lactic acid, an acid metabolite, which may cause long term and chronic stimulation to the tissue around the scaffold. Consequently, it may induce and aggravate inflammatory reaction and delay vascular healing [3]. Considering the above interpretations, it may eventually lead to slow development of PLLA scaffold and the de-listing of Abbott BVS scaffold [4]. In order to improve the biocompatibility and mechanical properties of PLLA, our study for the first time added nano-scale amorphous calcium phosphate (ACP) into PLLA to form a new-type vascular scaffold blended by bioceramic and polymer. ACP is a bioceramic material featured by high hardness, good biological activity, good biocompatibility, and strong cell affinity [5, 6]. Previous experiment of our research group proved that PLLA/ACP scaffold has better support performance than PLLA scaffold [7, 8]. However, it remains to be clarified whether long-term composite scaffold implantation can cause inflammation and calcification of vascular tissues around the scaffold. In this study, PLLA scaffold and biological scaffold synthesized with calcium phosphate were implanted into porcine coronary artery to observe and explore their effects on inflammation and calcification of vessels around the scaffold.

2. Materials and Methods

2.1. Scaffold Preparation. The host material of PLLA/ACP scaffold is the complex consisting of PLLA, and ACP. ACP (Ca/P = 1 : 1, size < 150 nm) was homogeneously mixed with PLLA powder (MW = 250,000 g/mol, Purac Biomaterials, Lincolnshire, IL, USA) with a ratio of PLLA/ACP at 98/2 (w/w) using a speed mixer (SpeedMixer™ DAC 600). The mixture was dried at around 60°C overnight prior to extrusion in a single screw extruder (Genca Engineering Inc., Saint Petersburg FL). The extruded tubes were laser-automated according to design specifications (3.0 mm diameter × 13 mm length × 150 μm width), and one radiopaque metal marker was incorporated one on each end. All scaffolds were crimped on 3.0 mm × 15 mm balloon catheters and sterilized with gamma radiation prior to implantation. The PLLA scaffold (3.0 mm diameter × 13 mm length × 150 μm width) was used for the control group; both the production process and the design of PLLA scaffold are as same as the PLLA/ACP scaffold [9].

2.2. Animal Preparation and Scaffold Implantation. Twenty-four minipigs aging 12-20 months and weighing 25-30 kg (no limitation in gender) were used in the experiment. The pigs were fed separately for more than 1 month before the experiment and orally administrated with 300 mg/d aspirin enteric-coated tablets and 75 mg/d clopidogrel hydrogen sulfate tablets 3 days before the experiment. Animal study protocol was approved by Institutional Animal Care Committee at Renmin Hospital of Wuhan University. All procedures involving animal use were conformed to the "Guide for the Care and Use of Laboratory Animals" published by the US National Institutes of Health [10].

Drinking water and food were deprived 12 hours before surgery. Basic anesthesia was performed by intramuscular injection of ketamine hydrochloride, midazolam, and scopolamine. Intraoperative anesthesia was achieved by intravenous anesthesia of ketamine combined with propofol. A 6F sheath was inserted into the femoral artery, the guide wire was pulled out, and 6,000 U heparin was injected. The angiographic catheter was inserted along the guide wire and hooked to the coronary artery, and multiposition angiography was performed. Two straight vascular segments of the left anterior descending branch, the left coronary circumflex branch, and the middle segment of the right coronary artery were randomly selected as the scaffold placement sites. Each pig was implanted with two PLLA/ACP scaffolds or two PLLA scaffolds. Three days after surgery, 1.6 million U penicillin BMP-2ium was intramuscularly injected to prevent infection. Aspirin enteric-coated tablets (100 mg) and clopidogrel hydrogen sulfate tablets (75 mg) were orally administrated continuously until the end point.

2.3. Hematological Examination. By venipuncture, 2 ml blood was collected for hematological examination before and 1, 6, 12, and 24 months after scaffold implantation. Serum levels of C-reactive protein (CRP, mg/l), calcium (Ca, mmol/L), and alkaline phosphatase (ALP, U/L) were measured using an automatic biochemistry analyzer (AU5400, Siemens, Germany) according to the manufacturer's instructions.

2.4. Intravascular Ultrasound. At each time point after angiography, 20 μg nitroglycerin was intracoronarily injected. The intravascular ultrasound (IVUS) catheter was inserted into the distal vessel at least 10 mm away from the scaffold along the guide wire, and then, the IVUS catheter was withdrawn automatically at 0.5 mm/s to record images. Image recording was performed every 2-3 mm to determine the relative position of the IVUS catheter and angiographic images. All IVUS images were recorded and saved for subsequent offline analysis. Each scaffold segment was divided into three segments in average: proximal, middle, and distal scaffold segment. Single-frame image of each segment was evaluated using vascular calcification score (Table 1). In each segment, the frame with the highest score was selected for calcification scoring, and finally, the average of three segments was used as the calcification score of this scaffold.

2.5. Animal Sampling and Pathological Examination. Three pigs in each group were sacrificed at the 1st, 6th, 12th, and 24th month after scaffold implantation, respectively. The scaffold segment was taken out, and partial tissue around the stented coronary was isolated and put into liquid nitrogen for cryopreservation for next molecular biological detection. The stented coronary sample was fixed with 10% formalin solution and embedded in paraffin.

The scaffold segment specimens were divided into proximal reference vessel, proximal scaffold, middle scaffold, distal scaffold, and distal reference vessel. The hard tissue was sliced using a slicer, and 5 sections were selected from each part for hematoxylin-eosin (HE) staining. Under a light

Table 1: Evaluation criteria for peri-strut coronary calcification score.

Degree/extent	<25%	≥25%, <50%	≥50%, <75%	≥75%
a	1	2	3	4
b	2	3	4	4
c	3	4	4	4

The calcification score is evaluated based on the degree and extent of calcification of the vessel wall structure by IVUS. Degree 0 = no calcification was found; a = internal elastic plate calcification of the blood vessel wall; b = calcification involved the medial membrane of the blood vessel; c = calcification involved the external elastic plate of the blood vessel wall. The extent (25%, 50%, 75%) refers to the portion of the circumference of the artery involved.

Table 2: Evaluation criteria for peri-strut inflammation score.

Degree/extent	<25%	≥25%, <50%	≥50%, <75%	≥75%
a	1	2	3	4
b	2	3	4	4
c	3	4	4	4

The peri-strut inflammation score is based on the degree of inflammation and extent of the circumference of the artery involved. Degree 0 = not present; a = scattered inflammatory cells; b = small and segmental aggregates of inflammatory cells; c = larger aggregates widespread or circumferentially distributed. The extent (<25%, 25%-50%, and >50%) refers to the portion of the circumference of the artery involved. In general, inflammation scores of 1 and 2 denote excellent local biocompatibility, namely, if neutrophils are not seen. An inflammation score of 3 or 4 may denote a biocompatibility issue, especially if neutrophils or large numbers of lymphocytes are present. Large proportions of eosinophils and lymphocytes may be indicative of a hypersensitivity response.

microscope, four quadrantic visual fields were selected from each section for observation. Under a microscope (magnification, ×40 and ×200), the inflammatory reaction around the scaffold was evaluated using inflammation score (Table 2).

In some sections, NF-κB was stained with immunohistochemistry to observe the inflammatory reaction, and some were subjected to ALP staining by immunohistochemistry to observe the calcification around the scaffold. Four visual fields were photographed in each section, and the percentage and average optical density of positive cells in the visual fields were randomly measured using the Image-pro Plus 6.0 image analysis system. Finally, positive expression = the percentage of positive cells × average optical density × 100.

2.6. Molecular Biological Detection. At the same time, the tissue around the scaffold was homogenated and detected by Western blot. The optical intensity of the electrophoretic band of IL-6 and BMP-2 was analyzed by a gel scanner. The expression levels of IL-6 and BMP-2 in muscle tissue were determined by the ratio of the optical intensity of the electrophoretic band of IL-6 and BMP-2 to the optical intensity of the electrophoretic band of β-actin, respectively.

2.7. Statistical Analysis. All results were analyzed by two independent observers. Data were presented as mean value ± standard deviation (SD). The differences between two groups were compared using independent two-sample t-test. The differences between time points were tested for the statistical significance using ANOVA followed by Tukey's test. $P < 0.05$ was considered statistically significant. All statistical analyses were performed with SPSS version 19.0 (Statistical Product and Service Solutions Ltd.).

3. Results

3.1. General Condition. All the 24 pigs survived healthy until the end point of sampling, and no major adverse cardiovascular events such as thrombus and myocardial infarction occurred after scaffold implantation.

No statistically significant differences were found in CRP, Ca, or ALP contents in blood between the two groups before and 1, 6, 12, and 24 months after scaffold implantation ($P > 0.05$, Table 3). The results demonstrated that neither PLLA scaffold nor PLLA/ACP scaffold caused obvious inflammatory reaction or calcification in the pigs after implantation [11].

3.2. Local Inflammation. In the PLLA group, at the 1st, 6th, 12th, and 24th month after scaffold implantation, HE staining showed that with the extension of implantation time, increasing infiltrated inflammatory cells were found around the PLLA scaffold (Figure 1). Inflammation scores increased gradually after scaffold implantation ($P < 0.05$, Figure 2). The IL-6 expression in the homogenate increased gradually after scaffold implantation ($P < 0.05$, Figure 2), and the IL-6 expression at the 6th, 12th, and 24th months after scaffold implantation was significantly higher than that at the 1st month after implantation ($P < 0.05$, Figure 2). At the 1st, 6th, 12th, and 24th month after scaffold implantation, NF-κB staining results showed that inflammatory cells were found around the PLLA scaffold (Figure 3).

In the PLLA/ACP group, no significant difference was found in the IL-6 expression among different time points after scaffold implantation ($P > 0.05$, Figure 2). There were a small amount of inflammatory cells around the scaffold at each time point, but the inflammation score, NF-κB positive index, and IL-6 expression had no significant differences at each time point ($P > 0.05$).

The infiltration of peripheral inflammatory cells in the PLLA group was significantly more obvious than that in the PLLA/ACP group (Figure 1). Inflammation score in the PLLA group was significantly higher than that in the PLLA/ACP group at the 12th and 24th months after scaffold implantation ($P < 0.05$, Table 4). The positive expression of NF-κB in the tissue and cells around the PLLA scaffold was significantly higher than that in the PLLA/ACP group at the 12th and 24th month after scaffold implantation ($P < 0.05$, Table 4). At the 6th, 12th, and 24th months after scaffold implantation, the IL-6 expression in the PLLA group was significantly higher than that in the PLLA/ACP group ($P < 0.05$, Figure 2).

3.3. Local Calcification. In the PLLA/ACP group, at the 1st, 6th, 12th, and 24th months after scaffold implantation revealed that ALP-rich cells were found around the PLLA scaffold (Figure 4). ALP positive index, BMP-2 expression,

Table 3: Serum level of CRP, Ca, and ALP.

	Preimplant	1 month	6 months	12 months	24 months
CRP (mg/l)					
PLLA	4.34 ± 1.39	4.73 ± 1.06	4.93 ± 0.97	5.16 ± 1.02	5.72 ± 1.49
PLLA/ACP	4.49 ± 1.37	4.64 ± 0.71	5.65 ± 0.84	5.24 ± 1.14	5.34 ± 1.14
P values	0.85	0.87	0.20	0.90	0.63
Ca (mmol/L)					
PLLA	1.36 ± 0.37	1.12 ± 0.31	1.16 ± 0.53	1.18 ± 0.35	1.28 ± 0.37
PLLA/ACP	1.36 ± 0.32	1.08 ± 0.26	1.11 ± 0.28	1.14 ± 0.41	1.21 ± 0.60
P values	0.98	0.80	0.85	0.85	0.81
ALP (U/L)					
PLLA	307.15 ± 60.08	307.68 ± 47.98	321.26 ± 59.22	313.33 ± 62.01	351.08 ± 47.21
PLLA/ACP	316.28 ± 54.45	288.93 ± 51.85	334.39 ± 54.07	354.44 ± 52.64	308.42 ± 59.26
P values	0.98	0.80	0.85	0.85	0.81

Data are presented as mean ± standard deviation. *P* values: PLLA/ACP group compared with PLLA group.

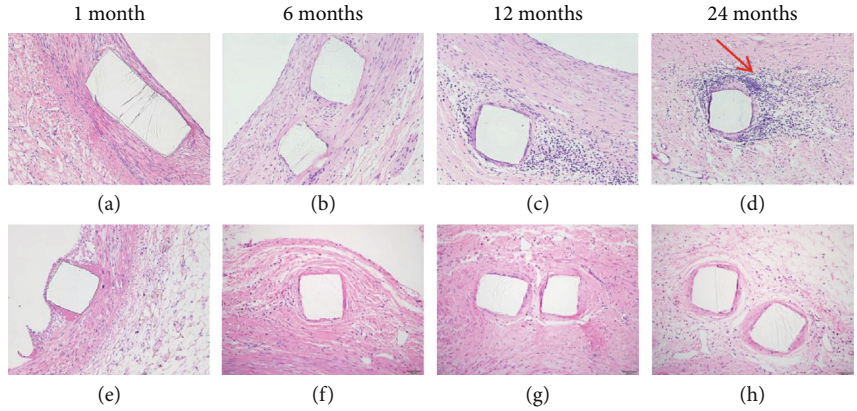

Figure 1: Hematoxylin-eosin staining. Histological cross-sections of the stented porcine coronary arteries from 1 month to 24 months (×200). (a–d) PLLA scaffolds and (e–h) PLLA/ACP scaffolds. Note the remarkable vascular wall swelling, tissue inflammation with PLLA scaffold (red arrows).

and calcification scores increased gradually after scaffold implantation, and ALP positive index, BMP-2 expression, and calcification scores increased gradually after scaffold implantation, and the BMP-2 expression at the 6th, 12 at the 6th, 12th, and 24th month after scaffold implantation was significantly higher than that at the 1st month after scaffold implantation ($P < 0.05$). In the PLLA/ACP group, no significant difference was found in ALP positive index and BMP-2 expression among different time points after scaffold implantation ($P > 0.05$, Figure 2).

The ALP positive expression around the PLLA scaffold was significantly higher than that in the PLLA/ACP group at the 6th, 12th, and 24th month after scaffold implantation ($P < 0.05$, Table 4). At the 12th and 24th month after scaffold implantation, the BMP-2 expression in the PLLA group was significantly higher than that in the PLLA/ACP group ($P < 0.05$, Figure 2). IVUS data showed no significant difference in calcification score between the two groups at the 1st and 6th month after scaffold implantation but higher calcification score in the PLLA group than the PLLA/ACP group at the 12th and 24th month after scaffold implantation ($P < 0.05$, Table 5).

4. Discussion

Nano-scale ACP is a biodegradable inorganic bioceramic material that has been widely used in biological and medical fields. ACP belongs to calcium phosphate family, which is a natural calcium and phosphate reservoir existed widely in nature. ACP is a calcium phosphate mineral that is nontoxic and harmless to the human body with weak alkaline property, possessing good hydrophilicity, tissue compatibility, and mechanical support as well [12, 13]. The major purpose of the addition of ACP is to increase the mechanical support performance of PLLA scaffold and reduce the thickness of the scaffold. It is expected to reduce the inflammatory reaction caused by acidic products during the degradation of PLLA scaffolds. However, considering ACP as a natural calcium and phosphate reservoir, it requires to be further explored whether long-term implantation of ACP may cause or

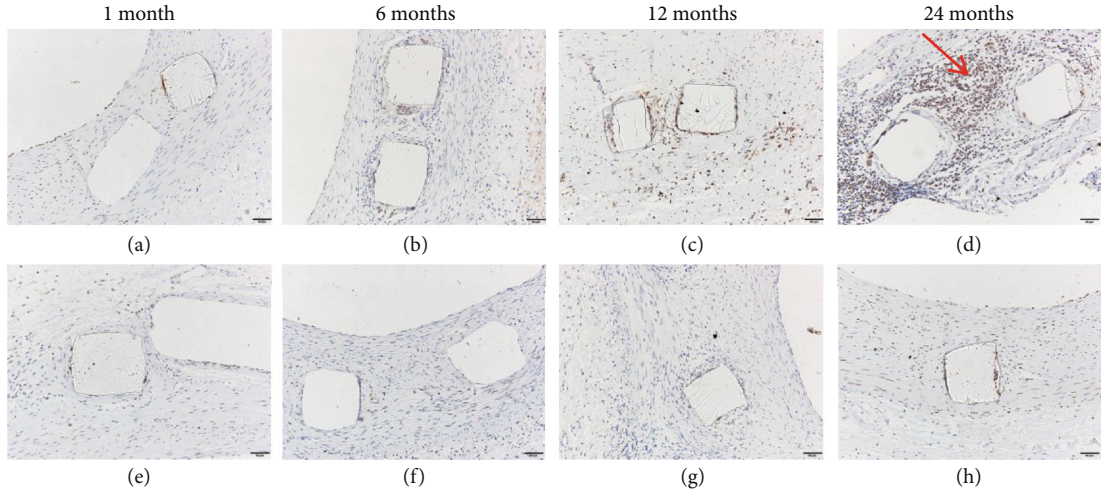

FIGURE 2: Immunohistochemistry staining of NF-κB, positive cells with the PLLA scaffold (a–d) and with the PLLA/ACP scaffold (e–h). Note the significantly lower expression of NF-κB in the PLLA/ACP stented artery (e–h) compared with that of the PLLA stented artery (a–d) (the red arrows show positive cells. ×200).

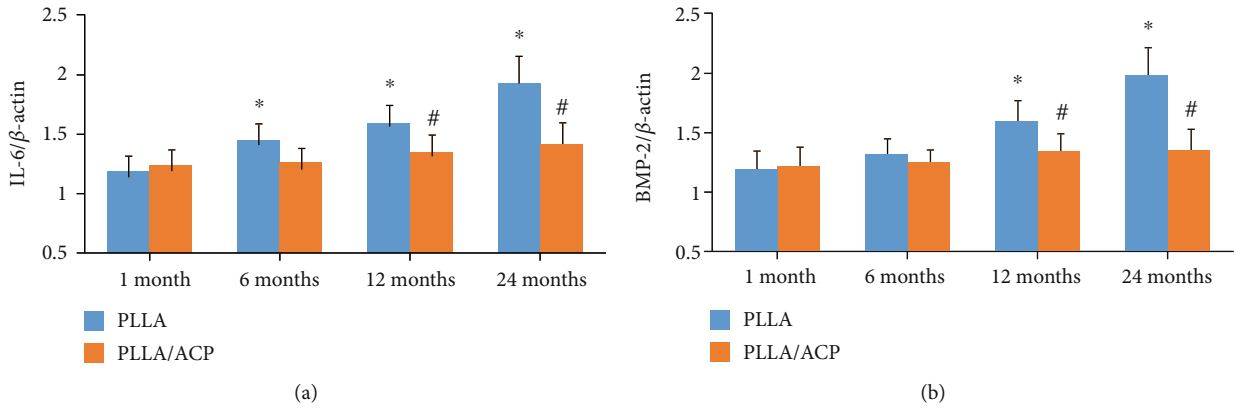

FIGURE 3: Western blotting analysis of coronary arteries treated with PLLA scaffolds and PLLA/ACP scaffolds for 24 months. The expression of IL-6 in the PLLA group was significantly higher than the PLLA/ACP group at 12 months and 24 months (a). The expression of BMP-2 in the PLLA group was significantly higher than the PLLA/ACP group at 6 months, 12 months, and 24 months (b). $P^* < 0.05$ means the PLLA group compared with the PLLA/ACP group. $P\#<0.05$ means that the data for 6 months, 12 months, and 24 months are compared with the data for 1 month.

promote calcification of tissues around the scaffold, affect the recovery of coronary systolic and diastolic function, even accelerate the formation of new atherosclerotic plaques of the diseased vessel in the scaffolding segment, thus resulting in serious end-stage cardiac events to patients with coronary heart disease. In this study, PLLA and PLLA/ACP scaffolds were implanted into porcine coronary arteries to explore the effect of PLLA/ACP scaffolds on inflammation and calcification of surrounding tissues at 1, 6, 12, and 24 months.

According to the results of this study, there was no significant difference in the content of CRP, calcium, and alkaline phosphatase between groups at 1, 6, 12, and 24 months after scaffold implantation, and there was no significant difference in the results of each group at each time point. It suggested that the two kinds of bioabsorbable scaffolds had no influence in systemic inflammation and calcification of experimental animals. In the aspect of inflammatory response, with the prolonged duration of scaffold implantation, the scaffold was continuously degraded and absorbed, showing increasingly more infiltration of inflammatory cells around the scaffold in the PLLA group, accompanied by gradual increase in inflammatory score, NF-κB positive expression index, and IL-6 expression level, which were obviously higher than those in the PLLA/ACP group at 12 and 24 months after implantation. It indicated that the addition of nano-scale ACP can significantly reduce local inflammatory response caused by PLLA scaffold degradation [14].

Furthermore, for calcification reaction, the scaffold was constantly degraded and absorbed with the prolonged duration of scaffold implantation. Besides, there were a growing number of calcification related reactive protein accumulation and potential calcification around PLLA scaffold. Meanwhile, calcification score, ALP positive expression index, and BMP-2 expression level increased gradually in the PLLA group and

Table 4: Pathology results.

	1 month	6 months	12 months	24 months
Inflammation scores				
PLLA	0.79 ± 0.41	1.33 ± 0.56	1.63 ± 0.58	1.92 ± 0.58
PLLA/ACP	0.80 ± 0.54	1.04 ± 0.46	1.13 ± 0.34	1.25 ± 0.53
P values	0.75	0.06	<0.01	<0.01
NF-κB positive index				
PLLA	27.97 ± 3.27	36.74 ± 4.24	42.49 ± 4.22	53.75 ± 5.63
PLLA/ACP	28.42 ± 3.81	32.59 ± 3.70	34.21 ± 6.51	37.41 ± 7.24
P values	0.82	0.10	0.03	<0.01
ALP positive index				
PLLA	39.61 ± 8.39	51.45 ± 6.21	61.32 ± 7.43	87.80 ± 9.29
PLLA/ACP	40.07 ± 10.08	43.21 ± 5.86	45.58 ± 6.14	51.71 ± 7.75
P values	0.93	0.04	<0.01	<0.01

Data are presented as mean ± standard deviation. *P* values: PLLA/ACP group compared with PLLA group.

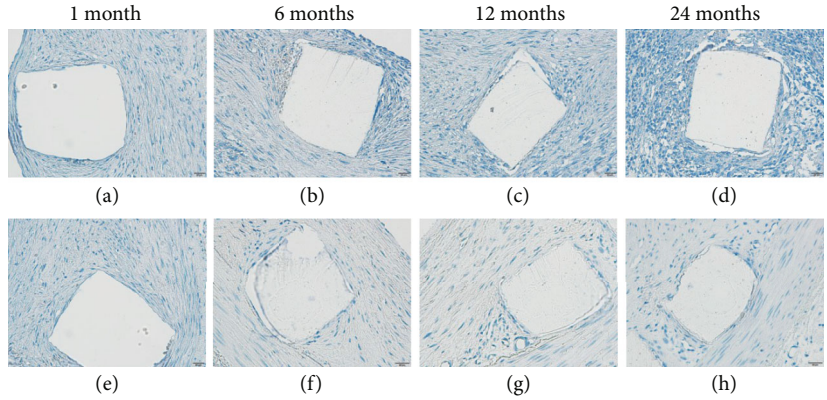

Figure 4: Immunohistochemistry staining of ALP, positive cells with the PLLA scaffold (a–d) and with the PLLA/ACP scaffold (e–h). Note the significantly lower expression of MMP-9 in the PLLA/ACP stented artery (e–h) compared with that of the PLLA stented artery (a–d) (×400).

Table 5: Calcification scores measured by IVUS.

	1 month	6 months	12 months	24 months
PLLA	0.17 ± 0.38	0.67 ± 0.48	1.21 ± 0.59	1.58 ± 0.50
PLLA/ACP	0.13 ± 0.34	0.50 ± 0.51	0.83 ± 0.48	1.04 ± 0.46
P values	0.69	0.17	0.02	<0.01

Data are presented as mean ± standard deviation. *P* values: PLLA/ACP group compared with PLLA group.

were significantly higher than those in the PLLA/ACP group at 12 and 24 months after implantation. In this regard, the addition of nano-scale ACP can significantly reduce the potential calcification of local tissue caused by PLLA scaffold degradation. One of the important factors of abnormal calcification of the body's soft tissues is the microinflammatory response, in which the chronic microinflammatory response of blood vessels leads to the formation of atherosclerosis. In the late stage of implantation of PLLA scaffold material, the expression levels of calcification-promoting factor alkaline phosphatase and BMP-2 in the tissue homogenate were higher than those of the PLLA/ACP scaffold material group, which indicates that PLLA scaffold material has certain calcification effect.

One of the important factors of abnormal calcification of soft tissue is the microinflammatory reaction, in which the chronic microinflammatory reaction of blood vessels leads to the formation of atherosclerosis that can also promote the abnormal calcification of soft tissue [15, 16]. The process of calcification promoted by microinflammatory reaction can be divided into three stages. To be specific, in the initial stage, inflammatory factors released by microinflammatory reaction and infiltrated monocyte/macrophage promote the formation of calcification factors in tissues. In the middle stage, the combination of microinflammatory response and calcification-promoting factor can transform histocytes into osteoblasts, secrete and release matrix vesicles, promote cell apoptosis, and release apoptotic bodies [17, 18]. In the case of high concentration of calcium and phosphorus, matrix vesicles and apoptotic bodies promote the formation of

hydroxyapatite and provide new focal points for its nucleation, thus forming microcalcification. In the later stage, the microinflammatory reaction further upregulates calcification-promoting factor, downregulates calcification-inhibiting factor, and promotes mineralization of stromal vesicles, resulting in the development of obvious tissue calcification from microcalcification [19].

With the addition of a small amount of ACP, it can be transformed into essential elements such as Ca and P through normal metabolism of human body and can bond with human tissue to form hydroxyl (-OH) group, generate a natural weak alkaline environment, neutralize acidic metabolites of PLLA, facilitate cell adhesion and growth, and thus reduce the occurrence of scaffold thrombosis and restenosis. In the process of alleviating inflammatory reaction, ACP also inhibits the potential effect of promoting calcification of PLLA degradable scaffolds. In view of the possible mechanisms, firstly, the local tissue develops acidic microinflammatory reaction that promotes calcification subsequently during the decomposition of PLLA, while the addition of weakly basic ACP material neutralizes acidic microinflammatory reaction of PLLA, thus reducing calcification. Secondly, ACP has a strong hydrophilicity [20, 21], which is conducive to the growth of cells, reducing cell apoptosis, thus decreasing the site of hydroxyapatite nucleation. Thirdly, the ratio of calcium to phosphorus in ACP is 1 : 1, with less content of calcium in ACP compared with other calcium phosphates with high ratio of calcium to phosphorus. Meanwhile, PLLA and ACP are mixed in the ratio of 98 : 2, forming a new bioabsorbable PLLA/ACP material that has less content of calcium and phosphorus, which can reduce the risk of calcification in the absence of high concentration of calcium and phosphorus.

5. Conclusions

To sum up, the novel bioabsorbable PLLA/ACP scaffolds have good histocompatibility and mild inflammatory response. In our study, the incorporation of small-dose ACP can reduce the acidic inflammatory response of PLLA scaffolds, which can not only maintain the formation of calcification in surrounding tissues but also inhibit tissue calcification by reducing the content of calcification-promoting factors in vivo.

5.1. Limitations and Future Studies. First, the coronary arteries of the experimental minipigs did not have atherosclerosis, and the inflammatory and calcification responses during vascular repair may be different from humans. Second, a relatively small sample size may affect the results of statistical analysis. We will carry out related research on the changes of ACP and PLLA materials on the biochemical environment around tissues. Our next step is to further extend to the atherosclerosis model and to detect and evaluate the effects of PLLA/ACP bioabsorbable scaffolds on the inflammation and calcification of surrounding tissues in the coronary intimal injury model.

Data Availability

All results were analyzed by two independent observers. Data were presented as mean value ± standard deviation (SD). The differences between two groups were compared using independent two-sample t-test. The differences between time points were tested for the statistical significance using ANOVA followed by Tukey's test. $P < 0.05$ was considered statistically significant. All statistical analyses were performed with SPSS version 19.0 (Statistical Product and Service Solutions Ltd.).

Conflicts of Interest

The authors declare that they have no conflicts of interest.

Acknowledgments

The study was supported by grants from the Wuhan Youth Science and Technology Chenguang Plan (2017050304010280), the NSFC Guidance fund project of the Renmin Hospital of Wuhan University (RMYD2018M24), and the Natural Science Foundation of Hubei Province (2020CFB238).

References

[1] Y. Sekimoto, H. Obara, K. Matsubara, N. Fujimura, H. Harada, and Y. Kitagawa, "Comparison of early vascular morphological changes between bioresorbable poly-L-lactic acid scaffolds and metallic stents in porcine iliac arteries," *Organogenesis*, vol. 13, no. 2, pp. 29–38, 2017.

[2] Z. Lan, Y. Lyu, J. Xiao et al., "Novel biodegradable drug-eluting stent composed of poly-L-lactic acid and amorphous calcium phosphate nanoparticles demonstrates improved structural and functional performance for coronary artery disease," *Journal of Biomedical Nanotechnology*, vol. 10, no. 7, pp. 1194–1204, 2014.

[3] S. Bangalore, H. G. Bezerra, D. G. Rizik et al., "The state of the absorb bioresorbable scaffold: consensus from an expert panel," *JACC: Cardiovascular Interventions*, vol. 10, no. 23, pp. 2349–2359, 2017.

[4] D. Mahtta and I. Y. Elgendy, "Everolimus-eluting bioresorbable vascular scaffolds: learning from the past to improve the future," *Minerva Cardioangiologica*, vol. 67, no. 4, pp. 288–305, 2019.

[5] D. R. Bienek and D. Skrtic, "Utility of amorphous calcium phosphate-based scaffolds in dental/biomedical applications," *Biointerface research in applied chemistry*, vol. 7, no. 1, pp. 1989–1994, 2017.

[6] Q. W. Fu, Y. P. Zi, W. Xu et al., "Electrospinning of calcium phosphate-poly (d,l-lactic acid) nanofibers for sustained release of water-soluble drug and fast mineralization," *International Journal of Nanomedicine*, vol. Volume 11, pp. 5087–5097, 2016.

[7] T. Dinh Nguyen, G. Feng, X. Yi et al., "Six-month evaluation of novel bioabsorbable scaffolds composed of poly-L-lactic acid and amorphous calcium phosphate nanoparticles in porcine coronary arteries," *Journal of Biomaterials Applications*, vol. 33, no. 2, pp. 227–233, 2018.

[8] G. Feng, J. Xiao, Y. Bi et al., "12-month coronary angiography, intravascular ultrasound and histology evaluation of a novel

fully bioabsorbable poly-L-lactic acid/amorphous calcium phosphate scaffolds in porcine coronary arteries," *Journal of Biomedical Nanotechnology*, vol. 12, no. 4, pp. 743–752, 2016.

[9] D. Gu, G. Feng, G. Kang et al., "Improved biocompatibility of novel biodegradable scaffold composed of poly-L-lactic acid and amorphous calcium phosphate nanoparticles in porcine coronary artery," *Journal of Nanomaterials*, vol. 2016, 8 pages, 2016.

[10] National Research Council (US) Committee for the Update of the Guide for the Care and Use of Laboratory Animals, *Guide for the Care and Use of Laboratory Animals*, National Academies Press (US), Washington (DC), 8th edition, 2011.

[11] H. Li, K. Sun, R. Zhao et al., "Inflammatory biomarkers of coronary heart disease," *Frontiers in Bioscience*, vol. 10, no. 1, pp. 185–196, 2018.

[12] J. N. O'Donnell, J. M. Antonucci, and D. Skrtic, "Amorphous calcium phosphate composites with improved mechanical properties," *Journal of Bioactive and Compatible Polymers*, vol. 21, no. 3, pp. 169–184, 2016.

[13] G. Feng, T. Dinh Nguyen, X. Yi et al., "Evaluation of long-term inflammatory responses after implantation of a novel fully bioabsorbable scaffold composed of poly-L-lactic acid and amorphous calcium phosphate nanoparticles," *Journal of Nanomaterials*, vol. 2018, 9 pages, 2018.

[14] J. D. Beck, K. L. Moss, T. Morelli, and S. Offenbacher, "Periodontal profile class is associated with prevalent diabetes, coronary heart disease, stroke, and systemic markers of C-reactive protein and interleukin-6," *Journal of Periodontology*, vol. 89, no. 2, pp. 157–165, 2018.

[15] L. Chen, H. Deng, H. Cui et al., "Inflammatory responses and inflammation-associated diseases in organs," *Oncotarget*, vol. 9, no. 6, pp. 7204–7218, 2017.

[16] M. Alique, R. Ramírez-Carracedo, G. Bodega, J. Carracedo, and R. Ramírez, "Senescent microvesicles: a novel advance in molecular mechanisms of atherosclerotic calcification," *International Journal of Molecular Sciences*, vol. 19, no. 7, p. 2003, 2018.

[17] K. Benz, K. F. Hilgers, C. Daniel, and K. Amann, "Vascular calcification in chronic kidney disease: the role of inflammation," *International Journal of Nephrology*, vol. 2018, 4310377 pages, 2018.

[18] P. S. Gade, R. Tulamo, K. W. Lee et al., "Calcification in human intracranial aneurysms is highly prevalent and displays both atherosclerotic and nonatherosclerotic types," *Arteriosclerosis, Thrombosis, and Vascular Biology*, vol. 39, no. 10, pp. 2157–2167, 2019.

[19] A. Sakamoto, R. Virmani, and A. V. Finn, "Coronary artery calcification: recent developments in our understanding of its pathologic and clinical significance," *Current Opinion in Cardiology*, vol. 33, no. 6, pp. 645–652, 2018.

[20] J. N. O'Donnell, G. E. Schumacher, J. M. Antonucci, and D. Skrtic, "Structure-composition-property relationships in polymeric amorphous calcium phosphate-based dental composites," *Materials (Basel)*, vol. 2, no. 4, pp. 1929–1954, 2009.

[21] S. Allegrini Jr., A. C. da Silva, M. Tsujita, M. B. Salles, S. A. Gehrke, and F. J. C. Braga, "Amorphous calcium phosphate (ACP) in tissue repair process," *Microscopy Research and Technique*, vol. 81, no. 6, pp. 579–589, 2018.